



# Modélisation et mesure des couplages en champ proche des composants de filtre CEM

Sanaa Zangui, Benjamin Vincent, Ronan Perrussel, Kévin Berger, Edith Clavel, Christian Vollaire, Carlos Sartori

## ► To cite this version:

Sanaa Zangui, Benjamin Vincent, Ronan Perrussel, Kévin Berger, Edith Clavel, et al.. Modélisation et mesure des couplages en champ proche des composants de filtre CEM. 2EMC, Nov 2010, Rouen, France. Proceedings of Embedded EMC, 2010. <hal-00538503>

**HAL Id: hal-00538503**

**<https://hal.archives-ouvertes.fr/hal-00538503>**

Submitted on 22 Nov 2010

**HAL** is a multi-disciplinary open access archive for the deposit and dissemination of scientific research documents, whether they are published or not. The documents may come from teaching and research institutions in France or abroad, or from public or private research centers.

L'archive ouverte pluridisciplinaire **HAL**, est destinée au dépôt et à la diffusion de documents scientifiques de niveau recherche, publiés ou non, émanant des établissements d'enseignement et de recherche français ou étrangers, des laboratoires publics ou privés.

# Modélisation et mesure des couplages en champ proche des composants de filtre CEM

S.Zangui, B.Vincent\*, R.Perrussel\*, K.Berger\*, E.Clavel\*\*, C.Vollaire\*, C.Sartori\*\*\*

Laboratoire Ampère – UMR CNRS 5005, Ecole Centrale de Lyon, 36 Avenue Guy de Collongue, 69130 Ecully, [sanaa.zangui@ec-lyon.fr](mailto:sanaa.zangui@ec-lyon.fr)

\* Laboratoire Ampère – UMR CNRS 5005, Ecole Centrale de Lyon, 36 Avenue Guy de Collongue, 69130 Ecully, [benjamin.vincent@ec-lyon.fr](mailto:benjamin.vincent@ec-lyon.fr), [ronan.perrussel@ec-lyon.fr](mailto:ronan.perrussel@ec-lyon.fr), [christian.vollaire@ec-lyon.fr](mailto:christian.vollaire@ec-lyon.fr)

\*\* Laboratoire G2Elab – UMR CNRS 5269, Site principal campus ENSE3 bat D 961, rue Houille Blanche BP 46, 38402 St Martin d'Hères Cedex, [edith.clavel@g2elab.grenoble-inp.fr](mailto:edith.clavel@g2elab.grenoble-inp.fr)

\*\*\* Escola Politécnica da Universidade de São Paulo LMAG/PEA/EPUSP, Av.Prof.Luciano Gualberto, Trav.3, N. 158. CEP- 05508-970- São Paulo,SP-Brasil, [sartori@pea.usp.br](mailto:sartori@pea.usp.br)

**Abstract :** EMC filters are increasingly integrated into power applications. To improve the filter performance it is important to model the electromagnetic interference between the components to optimize their positions. In this paper, a method is proposed to construct the equivalent model of the filter components. The proposed method is based on the multipolar expansion by representing the radiated emission of generic structures in a spherical reference ( $r, \theta, \varphi$ ). These models of the sources will be used to compute the mutual inductance between the components according to their geometric placement. Some results are presented illustrating our method.

**Index terms :** Electromagnetic compatibility (EMC), near-field, equivalent radiated source, multipolar expansion.

## 1. INTRODUCTION

EMC filters are designed to improve the electromagnetic compatibility and the immunity level of electric and electronic systems, in particular the aspects concerning power quality and electromagnetic signature. For this reason the filters performance has to be studied. Concerning these studies, the evaluation of the electrical parameters of the filter components plays an important role. Basically, there are two types of parasitic parameters: the self-parasitic parameters of the filter components and the mutual parasitic parameters that is related the coupling between components. Fig.1 represents the electric model of an EMC filter «  $\Pi$  » consisting of two capacitors  $C_{y1}$  and  $C_{y2}$ , and an inductance  $L_{DM}$ .

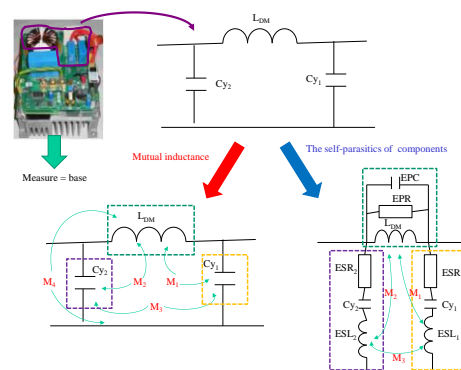


Fig.1 – Representation of a filter and the coupling and the self-parasitic parameters.

This model of filter includes the self-parasitic parameters and the inductive coupling between its components [1]. The capacitive effects are not considered, it can be justified based on the characteristic of the converters [1].

In Fig.1 the following notations are used:

- ESL, ESR, C: the self-parasitic parameters, inductance, resistance, and the capacitance,
- $L_{DM}$ , EPC, EPR: the inductance, and the related self-parasitic capacitance and the resistance,
- $M_1$  and  $M_2$ : mutual inductances between  $L_{DM}$  and the self-parasitic inductances  $ESL_1$  and  $ESL_2$ ,
- $M_3$ : mutual inductance between the self-parasitic inductances  $ESL_1$  and  $ESL_2$ ,
- $M_4$ : coupling inductance between  $L_{DM}$  and the Printed Circuit Board (PCB) tracks.

As Fig.2 shows how these parasitic parameters can affect the EMC filter performances. This figure was withdrawn from [2], and it presents three curves: the first one called “Base” represents the filter behavior before implementing the electromagnetic interference reduction and the filter performance improvement, the second “Minimized coupling” was obtained by optimizing the location of the components to reduce the coupling between filter components, and the third curve “Minimized coupling + ESL cancellation” represents the filter behavior after reducing the mutual parasitic and the effect of the equivalent serial inductance ESL.

The region A calls attention to the difference between the first curve “Base” and the second curve “Minimized coupling”, in particular to the first resonance frequency that matches the coupling effect of the filter components (mutual inductances). In a similar way, the region B represent the difference between the curves “Base” and the “Minimized coupling + ESL cancellation”, and the impact of the self-parasitic components.

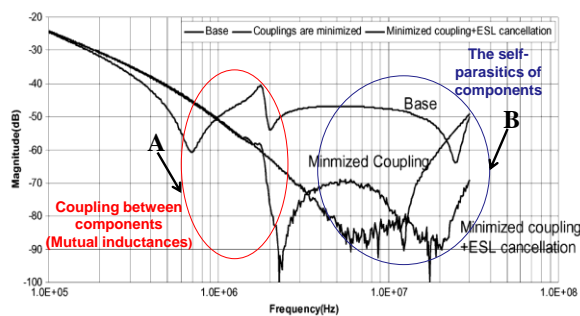


Fig.2 – Effect of parasitic parameters on EMC filter performance, extract from [2].

Thus, in a converter including passive and active components, the modeling of mutual parasitic components can be considered as a fundamental problem.

The objective of this work is to propose a methodology suitable for obtaining models that could represent the radiated field of the filter components, for a wide range of frequencies, useful to evaluate the filter performance. In particular, these models will be applied to determine the coupling effects between the filter components, basically the mutual inductance, considering the influence of parameters, such as the distance between components.

As the distance between components is much smaller than the wavelength related to the frequencies of power electronic applications, usually  $f < 100\text{MHz}$ , a quasi static approach can be considered. It is the case of a magnetic source, in which the capacitive effects are negligible.

The multipolar expansion is proposed to model the radiated field of the filter components. It can be used to represent the radiation of generic structures (coils, capacitors, tracks...).

This method can be used to compute the coupling effects between discrete components (capacitors, resistances and inductances) of power electronic devices. The global aim consists in simulating the whole configuration. Thus, the coupling between tracks should also be taken into account [3]. For this purpose, the Partial Element Equivalent Circuit (PEEC) method is used to determine the inductive and resistive effects (R, L, M) of PCB. For the parasitic capacitor evaluations, the MoM (Moments method) [4] and the Fast Multipolar Method FMM [5] are used. Our modeling allows integrating the equivalent sources by connecting them to the PCB track through circuit modeling.

## 2. METHODOLOGY

### a) Theory of the multipolar expansion

The multipolar expansion can be used to represent the electromagnetic fields in 3D, assuming that the field is computed outside a sphere of radius  $r$  that contains the equivalent source .

In the case of outgoing radiated emission source, the multipolar expansion allows expressing the electric and magnetic fields as [6]:

$$\mathbf{E}(r, \theta, \varphi) = \sum_{n=1}^{\infty} \sum_{m=-n}^n Q_{nm}^{TE} \mathbf{F}_{1nm}(r, \theta, \varphi) + Q_{nm}^{TM} \mathbf{F}_{2nm}(r, \theta, \varphi) \quad (1)$$

$$\mathbf{H}(r, \theta, \varphi) = \frac{j}{\eta} \sum_{n=1}^{\infty} \sum_{m=-n}^n Q_{nm}^{TM} \mathbf{F}_{1nm}(r, \theta, \varphi) + Q_{nm}^{TE} \mathbf{F}_{2nm}(r, \theta, \varphi) \quad (2)$$

Where

- $\eta = \sqrt{\frac{\mu}{\epsilon}}$  the intrinsic impedance of the considered environment.
- $Q_{mn}^{TE}$  and  $Q_{nm}^{TM}$  are the magnetic and electric multipoles, respectively. The coefficients  $Q_{mn}^{TE}$  describe the strength of the transverse-electric (TE) components of the radiated field, while coefficients  $Q_{nm}^{TM}$  describe the strength of the transverse-magnetic (TM) components. Each of them corresponds to the equivalent radiated source. Thus, these coefficients are the parameters to be identified to characterize the equivalent model of the radiated field components.
- $\mathbf{F}_{1nm}$  and  $\mathbf{F}_{2nm}$  are the vector spherical harmonics which are a solution of Maxwell's equations in free space, excluding the sphere that involves the sources. They are giving by:

$$\mathbf{F}_{1nm} = \mathbf{rot}(\mathbf{r} \cdot \Psi_{nm}) \quad \mathbf{F}_{2nm} = \frac{1}{k} \mathbf{rot} \mathbf{F}_{1nm} \quad (3)$$

The solution of the Helmholtz equation is then expressed as follows:

$$\Psi_{nm}(r, \theta, \varphi) = \frac{j}{\sqrt{n(n+1)}} b_n(kr) Y_{nm}(\theta, \varphi) \quad (4)$$

where  $Y_{nm}$  are the normalized spherical harmonics

$$Y_{nm}(\theta, \varphi) = \sqrt{\frac{(2n+1)(n-m)!}{4\pi(n+m)!}} P_n^m(\cos\theta) e^{jm\varphi} \quad (5)$$

In the aforementioned equations:

- $n$ : degree,
- $m$ : azimuthal order,
- $k$ : the phase constant,
- $r$ : distance from the center of the coordinate system,
- $b_n$ : The Bessel functions,
- $P_n^m$ : The Legendre associated functions.

In our study, the magnetic source in the near-field is considered. That is  $Q_{nm}^{TM} = 0$  and it is assumed that the electric field component is low when compared with the magnetic field. Thus, the determination of the  $Q_{mn}^{TE}$  (wrote  $Q_{nm}$  in the following) is carried out by radial the component  $H_r$ , in near field [6]:

$$H_r = -\frac{1}{4\pi} \sum_{n=1}^{+\infty} \sum_{m=-n}^n Q_{nm} \frac{\partial}{\partial r} \left( \frac{1}{r^{n+1}} \right) \cdot Y_{nm}(\theta, \varphi) \quad (6)$$

One of the main properties of the multipolar expansion to be emphasized is the decreasing of the order  $n$  terms with  $r^{-(n+1)}$ . This insures a hierarchy between each order of the decomposition. The larger the distance to the source is, the fewer are the terms required to reconstruct the field. In this way, the accuracy of the mutual inductance computation is related with the choice of the maximum order description, noted  $N_{max}$ . It should be observed that there are  $(2n+1)$  components for each  $n$  order. For an order source equal to  $N_{max}$ , it will correspond  $N_{max}(N_{max}+2)$  components, but due to the aforementioned property (hierarchy between each order),  $N_{max}$  can be limited, based on the present experience of the authors, up to 5.

#### b) Description of the methodology

A brief representation of the proposed methodology is presented in Fig.3. The method used to compute their mutual inductance is composed of two steps. The first one consists in determining the equivalent model of each component, independently of the other. This corresponds to  $Q_{nm}$  parameters. With these coefficients, the second step allows to calculate the mutual inductance, for example, between two components. Here, the difficulty consists to express all the multipoles in the same reference system.

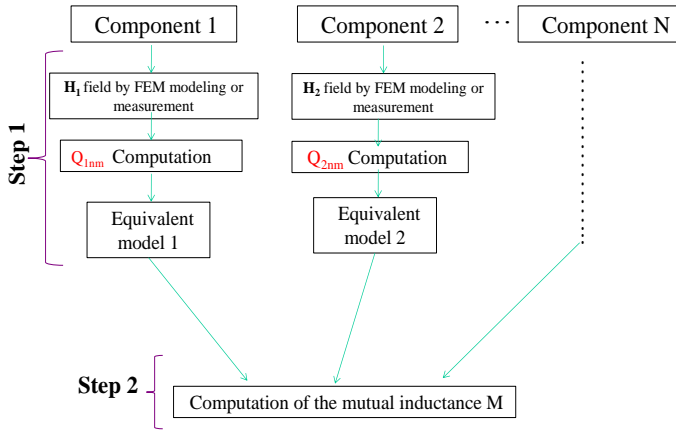


Fig.3 – Description of the methodology

### 3. FIRST STEP: MULTIPOLE IDENTIFICATION

Depending on the complexity of the object to model, we can calculate the radiated  $\mathbf{H}$ -field by using a 3D simulation model or by performing an experimental measurement [7]. Concerning the experimental results, some of the multipolar expansion components can be directly measured using magnetic induction sensors, for example, the sensors based on the standard CISPR16-1 coils [8].

#### a) Numerical approach used to identify the coefficients of the multipolar expansion

This approach consists to describe the component using simulations, for instance by a software based on the finite element method. Using the design of the source, the software calculates the radial component of induction on a measurement sphere  $S_M$  which contained this source, as shown in Fig.4. The determination of the  $Q_{nm}$  coefficients is achieved by integrating these components on  $S_M$ .

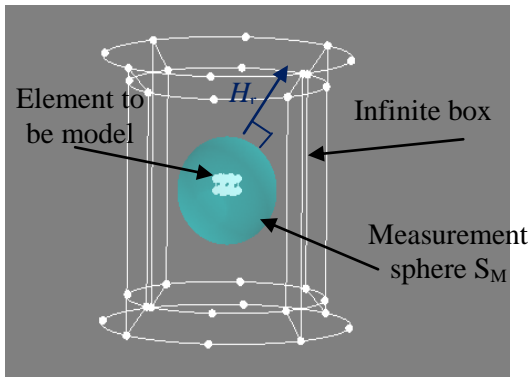


Fig.4 – Source modeling on Flux®

The coefficients of the multipolar expansion can be deduced from the equation (6), based on the expression:

$$Q_{nm} = 4\pi \frac{r_0^n}{(n+1)} \int_0^{2\pi} \int_0^\pi H_r(r_0, \theta, \varphi) \cdot Y_{nm}(\theta, \varphi) dS \quad (7)$$

Where  $H_r$  correspond at the radial components on the sphere  $S_M$  of a radius of  $r_0$ .

This result is due to the orthonormal property of  $Y_{nm}$  base:

$$\iint_{S_M} Y_{nm} \cdot Y_{n'm'} \cdot dS = \begin{cases} r_0^2 & \text{if } (n, m) = (n', m') \\ 0 & \text{if } (n, m) \neq (n', m') \end{cases} \quad (8)$$

There is no order limit for this identification method. But, the computational time increases with order  $n$ . Moreover, the discretization of the sphere surface has to respect the Shannon theorem in order to avoid problems with spatial aliasing. For example, with  $n = 1$ , two points are necessary for each direction in  $\theta$  and  $\phi$  axes. For  $n = 2$ , four points, etc. For  $N_{max}$  case, we will need  $2N_{max}$  points for each coordinate of the system.

Due to the complexity of the source, the implementation of this modelling can take very time and computational memory consuming. As an alternative method, a measured approach can be recommended, like the one detailed in the next section.

#### b) Measurement approach used to identify the components of the multipolar expansion

The approach used to identify the components of the multipolar expansion consists in measuring the magnetic flux coupled with large coils placed around the device in order to achieve a spatial integration. The measurement principle is similar to a spatial filtering: according to the coil shape, each sensor is sensitive to one specific component of the multipolar expansion [7]. A first prototype is shown in Fig.5.



Fig.5 – The prototype to identify the terms of the multipolar expansion [7].

The basic principle is to measure the magnetic flux through different coils in short circuit mode on the measurement sphere  $S_M$  (radius  $r_0$ ) around the device. The flux across the surface delimited by the set of coils is expressed by:

$$\begin{aligned} \mathbf{Flux}_{nm} &= \iint_{\text{coil surface}} (\mu_0 \cdot \mathbf{H}(r_0, \theta, \varphi) \cdot \mathbf{n}) ds \\ &= \frac{\mu_0}{4\pi} \frac{(n+1)}{r_0^{n+2}} Q_{mn} \iint_{\text{coil surface}} Y_{nm}(\theta, \varphi) dS \end{aligned} \quad (9)$$

Where  $\mathbf{n}$  is the unit outgoing normal of  $S_M$ , and  $\mathbf{Flux}_{nm}$  corresponds to the sum of the fluxes through the sensor coils. For example, in Fig.5, the  $Q_{10}$  sensor is composed by two coils. Thus,

$$\mathbf{Flux}_{nm} = flux_{10,1} + flux_{10,2} \quad (10)$$

Theoretical design and numerical validation has been presented [9]. This study shows that it was possible to create sensors in order to identify all the components of the first and second orders (8 components at all, 3 for  $n=1$  and 5 for  $n=2$ ).

The first prototype has been presented in [7]. It allowed measuring the z-dipole ( $Q_{10}$ ) and z-quadrupole ( $Q_{20}$ ) components of the equivalent magnetic multipole. It can be obtained based on the coil current measurements and the transfer function given by calibration of each loop antenna. Table 1 shows some results related to these source identifications. Sources are centered and their effects on the sensors are measured one after the other. In all cases, the consistent results validate the  $Q_{10}$  and  $Q_{20}$  theoretical values.

Thus, when the source is composed of a z-dipole, the result from the  $Q_{20}$  sensor measurement is very small. The proposed solution exhibits good filtering of the second order. This filtering capability is less significant for the z-quadrupole case. Indeed, current intensities are close to the sensitivity limits of the oscilloscope, so the accuracy is reduced.

It should be noted in Table I that the result of the calibration using the z-dipole is fairly good, with only 1.3% error.

	z-dipole source (mA.m <sup>2</sup> )		z-quadrupole source (mA.m <sup>3</sup> )	
	Calculated	Measured	Calculated	Measured
$Q_{10}$ sensor	7.854	7.955	/	-0.025
$Q_{20}$ sensor	/	$9.2 \cdot 10^{-4}$	0.732	0.753

Table 1. Identification results with two different sources placed at the center

A second prototype has been developed, and is under construction. A photo of the sensor system is presented in Fig.6. It allows getting the complete magnetic dipole (3 parameters): Two of them directly by the first measure and the third one by rotating the source of 90° around the z-axis.

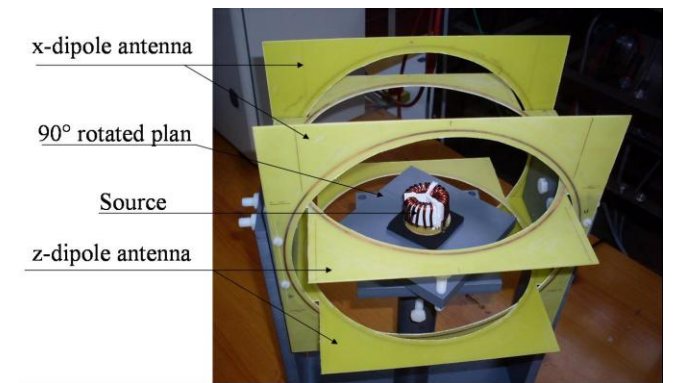


Fig.6 – Second prototype to identify the dipole terms of the multipolar expansion.

Once the equivalent source is obtained, it will be part of a component library, and it could be used in circuit simulators. That is, each component is

related to a specific electromagnetic signature corresponding to the radiated source.

#### 4. SECOND STEP: COMPUTING THE MUTUAL INDUCTANCE

##### a) Mutual inductance

Using the equivalent radiated field source model, we can determine the coupling between two equivalent sources through the computation of the mutual inductance. Fig.7 illustrates the configurations regarding the representation of two radiating sources (Models 1 and 2).

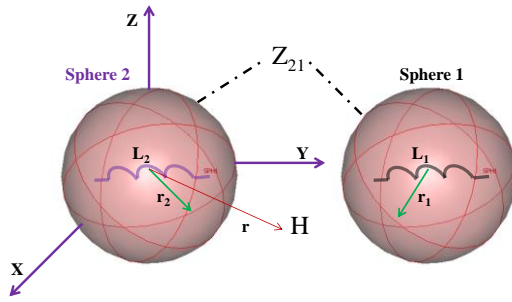


Fig.7 – Representation of two radiating sources.

The computation of the mutual impedance between source 1 and source 2 can be expressed in terms of the electrical field  $\mathbf{E}$  and magnetic field  $\mathbf{H}$  for each source, by [6]:

$$Z_{12} = -\frac{1}{i_1 i_2} \iint_{\Sigma_1} (\mathbf{E}_1 \times \mathbf{H}_2 - \mathbf{E}_2 \times \mathbf{H}_1) \quad (11)$$

When the spheres which contain each of the sources do not intersect, the mutual inductance can be expressed according to the coefficients of the multipolar expansion [6]:

$$M_{12} = \frac{1}{j\omega i_1 i_2} \frac{1}{k^2} \sqrt{\frac{\epsilon_0}{\mu_0}} \sum_{n=1}^{N_{max}} \sum_{m=-n}^n (-1)^m (Q_{1n,-m} * Q_{2nm}) \quad (12)$$

The coefficients associated to the magnetic transverse modes of the multipolar expansion of sources 1 and 2 must be expressed in the same reference: a translation is required, e.g. the

coefficients of the source 2 can be expressed in the reference of the source 1.

#### 5. NUMERICAL VALIDATION

To validate the method of computing the mutual inductance between two equivalent radiated sources of the components, the analytical result was compared to the numerical result computed by Flux® [10]. For this proposal, two similar loops configuration were considered,  $C_1$  and  $C_2$  with a radius “ $R_{spire}$ ” of 10 cm, separated by  $r$ , both located on the Oz-axis as shown in the Fig.8.

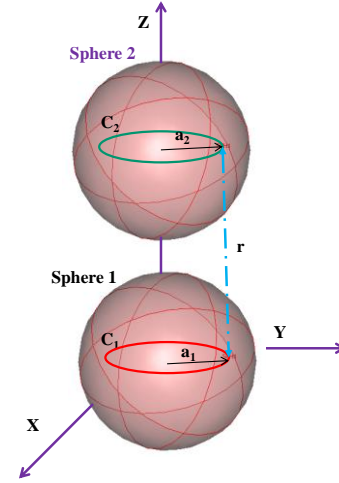


Fig.8 – Two similar coils placed on the z axis

In this case, the method of computing the mutual inductance in Flux® is based on the computation of the flux through the surface of one of the two loops.

We have computed the mutual inductance between the loops, according to the distance  $r$  using the method of spherical harmonics for  $n=3$  and  $n=5$ , and on the simulation of the flux through the surface of one of the two loops. The result is compared with those computed directly by Flux®. The comparison between the results is shown in the Fig.9.

To use the equivalent models of each loop to compute the mutual inductance, it is important that spheres included each source don't intersect, for that reason a minimum distance equal to  $(R_{coil1} + R_{coil2}) = 0.2m$  between their centers must be respected.

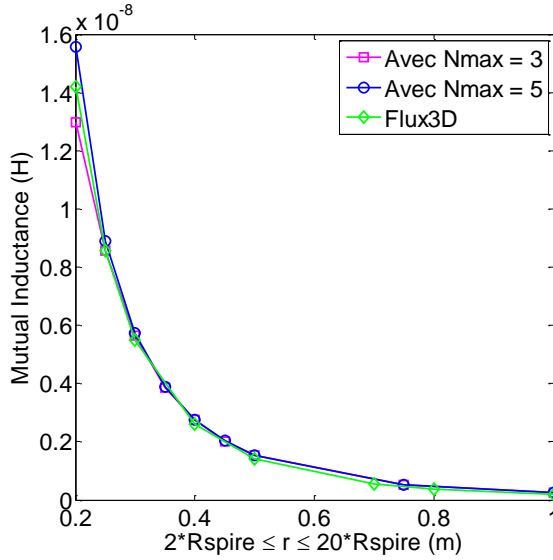


Fig.9 – The comparison between spherical harmonics mutual inductance result and Flux® up to the near-field distance limit at 200MHz (1m)

As shown in Fig.9, the results between the method using a truncated multipolar expansion and the numerical method in Flux® are comparable.

To compute the mutual inductance for a small distance between the two loops, the number of terms required to describe the complexity of the source increases. For that reason, at distance of  $r=0.2m$  the error is greater for  $n=3$  than  $n=5$  as show in the Fig.10.

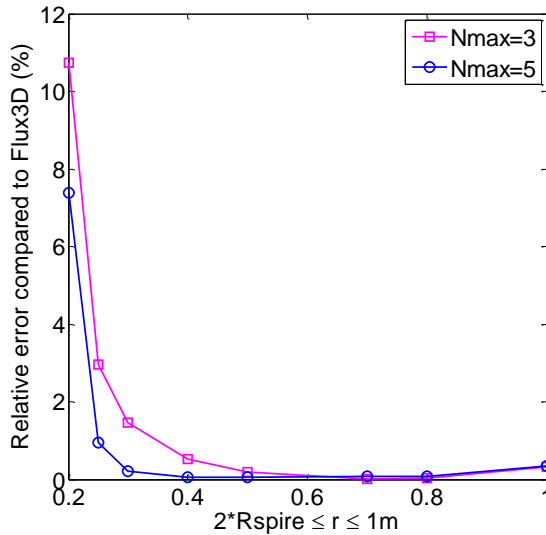


Fig.10 – The relative error compared to FEM result

## 6. PROPOSED MEASUREMENT METHOD

The method for measuring the mutual inductance between two loops C1 and C2, of inductors L1 and L2 is based on the measurement of the coefficient of coupling K. The coefficient of coupling is expressed in function of the inductors L1 and L2, the input and output voltage by the following relation [11]:

$$K = \frac{M}{\sqrt{L_1 \cdot L_2}} = \frac{\sqrt{L_1}}{\sqrt{L_2}} \cdot \frac{V_S}{V_E} \quad (13)$$

$K$ : coefficient of coupling,  
 $M$ : mutual inductance,  
 $V_S$ : input voltage,  
 $V_E$ : output voltage.

This relation is valid when  $L_1\omega > 10 \cdot R$  [11], with R the resistance of the loop. For this reason, it is interesting to study the behavior of the impedance of loop in function of frequency.

This method will be used in the case of two identical loops located on the Oz-axis to measure the coefficient of coupling in function of the distance r between the two loops.

## 7. CONCLUSION

The presented methodology enables the evaluation of coupling parameters of EMC filter components by using equivalent emission sources. This method is composed by two steps. At first, the equivalent sources which represent the radiated field component using the multipolar expansion representation are identified. It can be obtained by a numerical or an experimental approach. Both of them were discussed in the paper. Secondly, the equivalent sources will be used to compute the coupling between them, which was represented by a mutual inductance as a function of the distance that separates them.

Although some simple configurations were used to validate the proposed methodology, some non canonical structures are planned to be evaluated by the authors in the near future. Moreover, other kind of multipolar expansions, like the cylindrical one can be more suitable for modeling components such as tracks or cables, and it will also be considered. For example, in the case of the coupling between a track and a component, the spherical harmonics

method is not very adequate and other harmonics method should be used.

The method proposed could be helpful when used together with other circuit simulator methods in the evaluation of equivalent circuit of power electronics devices (R-L-M-C). This will give us a considerable gain of memory space concerning the full model configuration used in EMC filter numerical simulations.

## 8. ACKNOWLEDGMENT

This work was supported in part by the competitive cluster MOVEO (project O2M) and the CAPES-COFECUB (project 568/09).

## 9. REFERENCES

[1] S.Wang, F.C.Lee and W.G.Odendaal, "Controlling the parasitic parameters to improve EMI filter performance", 2004 IEEE, National science foundation under Award Number EEC-9731677.

[2] S.Wang, F.C.Lee and W.G.Odendaal, "Cancellation of capacitor parasitic parameters for noise reduction application", IEEE Transactions on power electronics, Vol.21, No.4, July 2006.

[3] V.Ardon, O.Chadebec, E. Clavel, J-M. Guichon, E. Vialardi V. "EMC Modeling of an Industrial Variable Speed Drive with an Adapted PEEC Method", COMPUMAG, Florianopolis, Brazil, 22-26 Nov 2009.

[4] R. F. Harrington, Field Computation by Moment Methods. New York: Macmillan, 1968.

[5] H. Cheng, L. Greengard, V. Rokhlin, "A Fast Adaptive Multipole Algorithm in Three Dimensions", Journal of Computational Physics 155, 468-498 (1999). Article ID jcph, 1999, 6355, available at <http://www.idealibrary.com> on IDEAL®

[6] Billy C.Brock « Using vector spherical harmonics to compute antenna mutual impedance from measured or computed fields », SANDIA Report, April 2001

[7] B. Vincent, O. Chadebec, J.-L. Schanen, K. Berger, « Loop antennas for Near Field Multipolar

*Expansion Identification: First experimental Validations* », to be published in ICONIC 2009 – Special Issue of IEEE Transactions on Instrumentation and Measurement.

[8] Standard CISPR 16-1, part P, 2002, pp.230-237 and 396-409.

[9] B.Vincent, O.Chadebec, J.-L.Shanen, C.A.F. Sartori and L.Krahenbühl, "New robust coil sensors for near field characterization", Journal of Microwaves, Optoelectronics and Electromagnetic Applications, Vol. 8, No. 1, pp.64S-77S, June 2009, article available on JMOE website: <http://www.sel.eesc.usp.br/jmo/>

[10] [www.cedrat.com](http://www.cedrat.com)

[11] D.PARET, « Applications en identification radiofréquence et cartes à puce sans contact », DUNOD, 2003, pp. 372-374.